JACS
JOURNAL OF THE AMERICAN CHEMICAL SOCIETY
Article
pubs.acs.org/JACS

Nature's Polyoxometalate Chemistry: X-ray Structure of the Mo Storage Protein Loaded with Discrete Polynuclear Mo−O Clusters

Björn Kowalewski,[†,§] Juliane Poppe,[‡,§] Ulrike Demmer,[‡] Eberhard Warkentin,[‡] Thomas Dierks,[†] Ulrich Ermler,*[,‡] and Klaus Schneider*[,†]

[†]Biochemie I, Fakultät für Chemie, Universität Bielefeld, Universitätsstraße 25, D-33615 Bielefeld, Germany
[‡]Max-Planck-Institut für Biophysik, Max-von-Laue-Straße 3, D-60438 Frankfurt am Main, Germany

Supporting Information

ABSTRACT: Some N_2-fixing bacteria prolong the functionality of nitrogenase in molybdenum starvation by a special Mo storage protein (MoSto) that can store more than 100 Mo atoms. The presented 1.6 Å X-ray structure of MoSto from *Azotobacter vinelandii* reveals various discrete polyoxomolybdate clusters, three covalently and three noncovalently bound Mo_8, three Mo_{5-7}, and one Mo_3 clusters, and several low occupied, so far undefinable clusters, which are embedded in specific pockets inside a locked cage-shaped $(\alpha\beta)_3$ protein complex. The structurally identical Mo_8 clusters (three layers of two, four, and two MoO_n octahedra) are distinguishable from the $[Mo_8O_{26}]^{4-}$ cluster formed in acidic solutions by two displaced MoO_n octahedra implicating three kinetically labile terminal ligands. Stabilization in the covalent Mo_8 cluster is achieved by Mo bonding to Hisα156−$N_{\varepsilon 2}$ and Gluα129−$O_{\varepsilon 1}$. The absence of covalent protein interactions in the noncovalent Mo_8 cluster is compensated by a more extended hydrogen-bond network involving three pronounced histidines. One displaced MoO_n octahedron might serve as nucleation site for an inhomogeneous Mo_{5-7} cluster largely surrounded by bulk solvent. In the Mo_3 cluster located on the 3-fold axis, the three accurately positioned His140−$N_{\varepsilon 2}$ atoms of the α subunits coordinate to the Mo atoms. The formed polyoxomolybdate clusters of MoSto, not detectable in bulk solvent, are the result of an interplay between self- and protein-driven assembly processes that unite inorganic supramolecular and protein chemistry in a host−guest system. Template, nucleation/protection, and catalyst functions of the polypeptide as well as perspectives for designing new clusters are discussed.

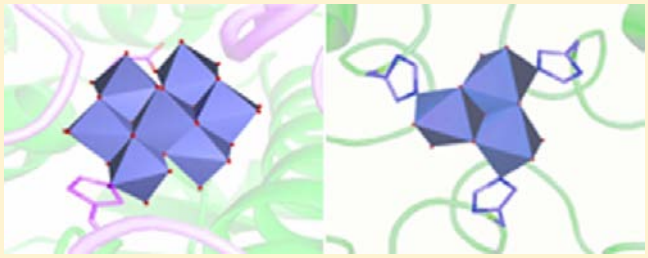

1. INTRODUCTION

In inorganic chemistry, molybdenum (Mo) actually attracted considerable attention because of its tremendously expanded Mo-dominated polyoxometalate (POM) chemistry[1−4] culminating in aggregates containing up to 368 Mo atoms, the largest inorganic molecules known to date.[5,6] The vast variety and size of polynuclear Mo−O (polyoxomolybdate) clusters are due to the flexibility of the Mo−O−Mo links, easy redox changes particularly between Mo^V and Mo^{VI} oxidation states, variable coordination numbers, the strong stabilization by hydration, and the capability to form chain terminating Mo=O bonds. Their diversity is further expanded in the presence of template type species or compounds inducing nucleation.[7−11] POM clusters of the Mo_7 and Mo_8 types are readily formed by rapid self-assembly processes in MoO_4^{2-}-containing aqueous solutions at pH 3−5.[12] The coordination number of Mo thereby increases from four (tetrahedral MoO_4^{2-} anion) to six (octahedral MoO_6 building blocks). In biology, Mo is required in special organometallic cofactors associated with redox enzymes that catalyze key steps in carbon, nitrogen, and sulfur cycles. For that, organisms had to develop a complex Mo metabolism including Mo uptake/transport, Mo processing for cofactor biosyntheses, gene regulation, intracellular Mo homeostasis, and Mo storage.[13−18] For all of these functions and processes, "Mo-binding proteins" are required, which are able to rapidly bind and release molybdate.[16]

The most unusual Mo-binding protein, discovered in 1981 in *Azotobacter vinelandii*,[19] termed Mo-storage protein (MoSto), is functionally related to nitrogen fixation by supplying nitrogenase with molybdenum, particularly when *Azotobacter* cells are cultivated under Mo starvation conditions.[16,20] Biochemical and structural analysis indicate that MoSto is an $(\alpha\beta)_3$ hexameric complex,[21] which shows no structural similarities with other Mo-proteins, neither molybdenum cofactor-containing enzymes such as Moco enzymes,[15] FeMoco nitrogenases,[22] or the "orange protein"[23] nor with members of the so-called Mod/Mop protein family ("molbindins") capable of binding up to eight monomolybdate ions.[13,14] Unexpectedly, MoSto exhibits a structure similar to those of nucleoside monophosphate kinases. The most related family member is the bacterial/archaeal hexameric UMP kinase, which phosphorylates UMP by hydrolysis of ATP.[24,25] Subunits α and β of MoSto (genetic designations: *mosA*, *mosB*[16]) are

Received: March 30, 2012
Published: May 22, 2012

   dx.doi.org/10.1021/ja303084n | *J. Am. Chem. Soc.* 2012, 134, 9768−9774

structurally highly similar and fold as an open $\alpha\beta$ structure consisting of an α,β core (six-stranded parallel β-sheet flanked by six α-helices) and two attached lobes (see Figure S1, Supporting Information). A groove between the C-terminal side of the central β-sheet and the corresponding lobe serves as the ATP-binding site. Biochemical studies indicate that incorporation of Mo into the apoprotein requires ATP.[26]

The storage protein is capable of binding more than 100 Mo atoms in vitro.[26] Alternatively, it can bind about the same number of tungsten (W) atoms in vitro due to the similar chemical properties of Mo and W at least in the highest oxidation state. Extended X-ray absorption fine structure data suggested that Mo and W are stored in the form of POM clusters.[16] In the case of the partially W-loaded storage protein (WSto), the presence of several polyoxotungstate clusters have, in fact, been proven by a recent X-ray structure.[21] However, because of their weak occupancy, only the structure of a W_3 cluster could unambiguously be analyzed. Metal storage of MoSto is also an example for a biomineralization process, a topic that attracted broad attention in the fields of nanomaterial science and biotechnology.[27] A related case has been described for ferritin or ferritin-like proteins housing huge amounts of nanosized iron oxide fragments.[28] However, the metal-uptake mechanism and the metal oxides formed in ferritins are fundamentally distinct from those of MoSto primarily due to the different nature of iron and molybdenum.

A structural characterization of MoSto in its physiological form loaded with polyoxomolybdate clusters is more complicated as they are distinctly less stable than polyoxotungstate clusters,[7] also in the protein-bound state.[21,26] In this Article, we describe the conditions for stabilizing MoSto in complex with polyoxomolybdate clusters, its structure at 1.6 Å resolution, and discuss general aspects of cluster composition/structure as well as a mechanism of protein-assisted POM cluster synthesis. MoSto is unique in biology and extends the competence of proteins, in general, by synthesizing/binding/protecting polynuclear metal−oxide clusters of different types.

2. RESULTS

Preparation and Overall Structure of MoSto Loaded with Molybdate. The established purification of MoSto from *A. vinelandii*[26] resulted in an average Mo content of ca. 60 atoms per MoSto molecule, which might be close to the average in vivo value. However, the Mo-binding capacity of MoSto could be nearly doubled in an in vitro experiment, when first the Mo-free apoprotein was produced under "release conditions" (incubation at pH 7.6 for 1 h at 30 °C) and then the holoprotein reconstituted after addition of 1 mM ATP, 1 mM $MgCl_2$, and 2 mM Na_2MoO_4.[26] On the basis of this finding, we have effectively chosen "reconstitution conditions" (presence of ATP, $MgCl_2$, and molybdate in all buffers) during the whole purification procedure (see Materials and Methods) resulting in a distinctly more stable protein and a higher yield of pure MoSto (17 mg from 2.4 L cell suspension). The highest Mo content measured includes up to ca. 130 Mo atoms/MoSto molecule. MoSto samples with maximal amounts of molybdate were applied for crystallization experiments performed at low temperatures of 4 or 10 °C where the polyoxomolybdate clusters are more stable.[26]

The determined crystal structure of native MoSto at a resolution of 1.6 Å (Table S1, Supporting Information) is highly related to that of WSto,[21] the rms deviation of the C_α atoms being 0.5 Å (Figure 1). Architecturally, MoSto is a cage-like $(\alpha\beta)_3$ protein complex with a cavity of ca. 7250 Å^3. Well-defined pockets on the surface of the cavity form the binding site for various POM clusters. Because the cavity of the structurally characterized protein appears to be completely locked from the outside, we termed this state as "closed state". This state is biologically relevant for long-term Mo storage as undesirable Mo release and protein destabilization is thus prevented. On the other hand, a second "open state" has to exist with a pore to allow molybdates to enter and exit the cavity. Although not structurally explored yet, a workable model of the open state is offered by the structurally related UMP kinase determined in a closed and open conformation,[24,25] which suggests, transferred to MoSto, the existence of two small pores along the 3-fold axis as entrance and exit for monomolybdates and dimolybdates (Figure 1). Polymerization of molybdates to larger POM aggregates as discovered in MoSto and described in detail in the following sections must, however, occur inside the cavity, because large clusters can neither be formed spontaneously under the crystallization conditions nor in solutions at physiological pH values.

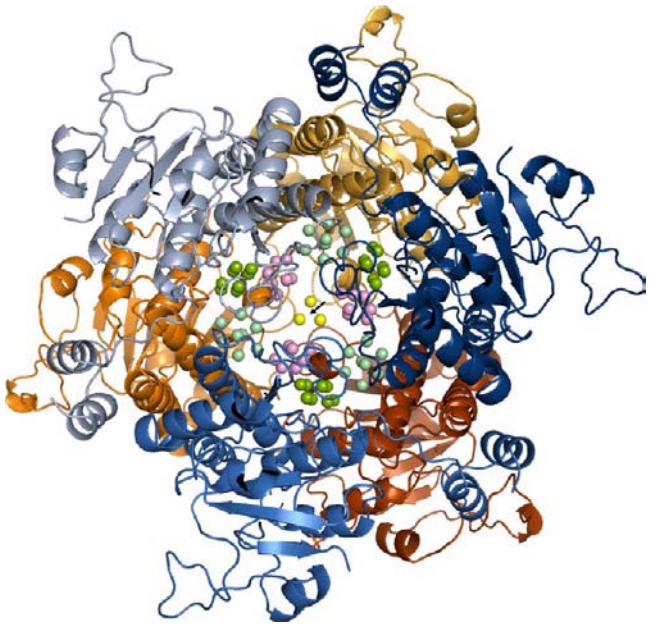

Figure 1. Structure of MoSto from *A. vinelandii* in a closed state. The heterohexameric $(\alpha\beta)_3$ protein complex (α subunit orange, β subunit blue) builds up a large occluded cavity in its interior. Pores across the protein shell are assumed at the interface of the three subunits α and β along the 3-fold axis (black arrow). The cavity is occupied by more than 100 Mo atoms in form of POM clusters (Mo_3 yellow, covalent Mo_8 cyan, noncovalent Mo_8 green, Mo_{5-7} magenta).

To correctly assign the type of each cluster atom in its corresponding position, we performed X-ray fluorescence scan and single anomalous dispersion experiments on MoSto crystals. Elements (like magnesium and phosphorus) with adsorption edges outside the wavelength spectra of the scan (0.6−2.1 Å) could be distinguished from Mo by their low anomalous dispersion signal at a wavelength of 1.73 Å. Accordingly, from ca. 130 Mo atoms determined to be protein-bound in solution prior to crystallization, ca. 70 Mo atoms were found in defined and ca. 30 Mo atoms essentially in undefined clusters of the structure. The residual molybdates were presumably disordered or lost during crystallization. The definable polynuclear Mo−O clusters (10 in total) were subdivided into four distinct types: one Mo_3 (trimolybdate)

dx.doi.org/10.1021/ja303084n | J. Am. Chem. Soc. 2012, 134, 9768−9774

cluster, located around the 3-fold axis, three Mo_{5-7} (penta-/hexa-/hepta-molybdate) clusters (one per $\alpha\beta$ dimer), and six in principle structurally identical Mo_8 (octamolybdate) clusters (Figure 1), which differ in the type of bonding to the polypeptide. Three of the Mo_8 clusters are covalently bound, and the other three noncovalently bound. In addition, we found two larger POM clusters along the 3-fold axis and a few smaller Mo−oxide aggregates with low occupancy and structural inhomogeneity that will be not discussed further. It is assumed that the same polyoxomolybdate types found in vitro are formed inside the cell.

The Mo_3 Cluster. The Mo_3 cluster (Figure 2A) is positioned in front of the coincidence point of the three α subunits on the 3-fold axis (Figure 2B). As reflected by the low temperature factor of 10.3 Å^2 for Mo (average temperature factor of MoSto 20.7 Å^2), the cluster site is completely occupied. The Mo_3 cluster consists of three triangularly arranged Mo atoms; the 3-fold symmetry axis between them corresponds to that of the $(\alpha\beta)_3$ protein complex. Each Mo atom is octahedrally coordinated to five O atoms and, unexpectedly, to the imidazole $N_{\varepsilon 2}$ atom of Hisα140. The distorted octahedra are edge-bridged, and the O atom that belongs to all three octahedra sits exactly on the 3-fold axis and points to the assumed exit of the cavity (Figure 2B). The resulting composition of the Mo_3 cluster is $[Mo_3O_{10}N_3(His)\text{-}H_n]^{n-2}$. In particular, the two terminal oxygen atoms are involved in POM cluster−polypeptide interactions (Figure S2A, Supporting Information). The first terminal oxygen atom of each Mo atom is hydrogen-bonded to Glnα136 and via a water molecule to Glnα129 and Thrα132. The second terminal oxygen atom points toward the side chain of Ileα139 and is perhaps protonated. Moreover, the three bidentate oxygen atoms interact via a water molecule to Glnα136 and Thrα132.

The Covalent Mo_8 Clusters. Three covalently bound octamolybdate clusters (one per $\alpha\beta$ dimer), referred to as covalent Mo_8 clusters (Figure 3A), are attached to flat and asymmetric pockets formed by residues of the α subunits (Figure 3B). Their occupancy is high and homogeneous as indicated by a uniform temperature factor of 10.6 ± 1.7 Å^2 for the eight Mo atoms. Topologically, the Mo_8 cluster represents a three-layer structure of two, four, and two MoX_n octahedra, which are displaced relative to each other by a half octahedron. In addition to its bonding to inorganic O atoms, the Mo_8 cluster is also coordinated to the proteinogenic ligands Hisα156 imidazol $N_{\varepsilon 2}$ and Gluα129 carboxylate $O_{\varepsilon 1}$ (Figure 3). The Mo_8 cluster of MoSto is related to the classical $[Mo_8O_{26}(OH)_2]^{6-}$ and $[Mo_8O_{26}]^{4-}$ clusters, which self-assemble in strongly acid solution,[7] but differs from them by a tangential displacement of two MoX_n octahedra, one of the first and one of the third layer, in opposite directions. As a consequence, these MoO_n octahedra become corner-bridged in the protein-bound Mo_8 cluster, and the thereby created three terminal oxygen atoms make these clusters kinetically labile.[29] (In the classical $[Mo_8O_{26}]^{4-}$ cluster, they are edge-linked implicating two terminal oxygen atoms.) The displaced MoX_n octahedra are stabilized in MoSto by replacing the third terminal ligand by the mentioned histidine and glutamate side chains (Figure 3). The resulting composition of the cluster is $[Mo_8O_{26}O(Glu)N(His)H_n]^{n-5}$. Accordingly, the covalent Mo_8 cluster of MoSto consists of 15 monodentate, six bidentate, four tridentate, and two tetradentate oxygen atoms as well as one monodentate nitrogen atom from Hisα140. The MoX_n octahedra are partly distorted against each other, resulting in

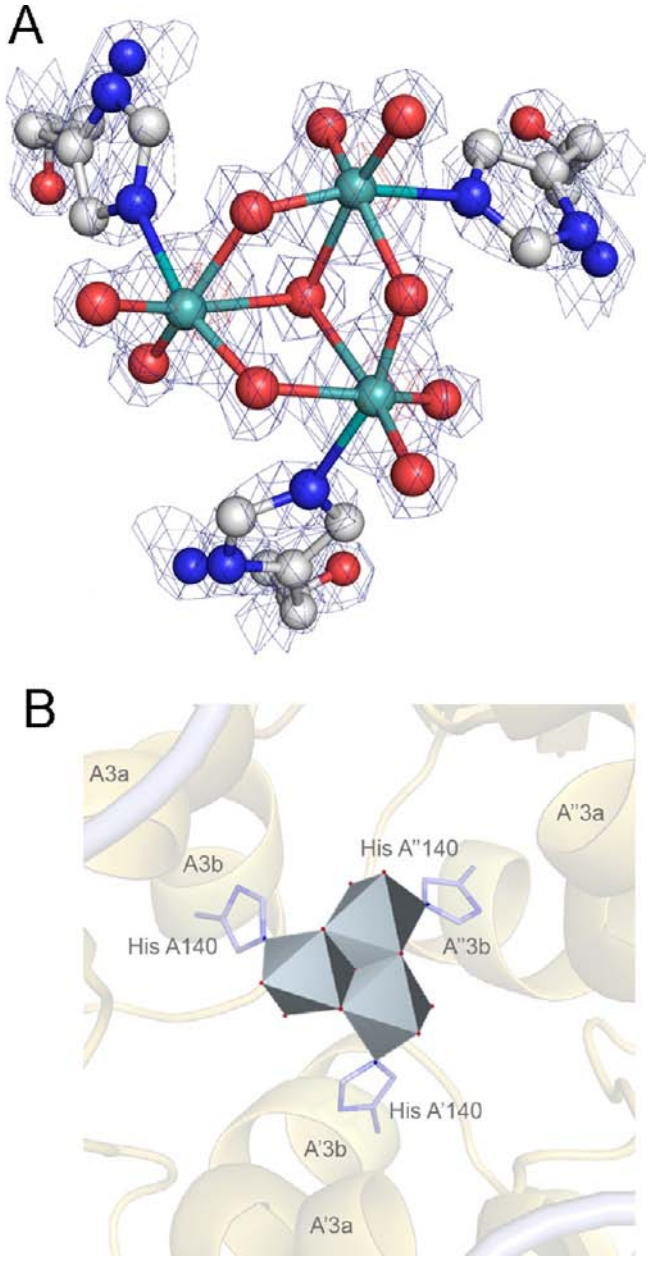

Figure 2. The Mo_3 cluster. (A) Structure (ball-and-stick representation) with electron density. Each Mo atom (cyan) is coordinated to five O atoms (red) and the $N_{\varepsilon 2}$ atom (blue) of Hisα140. The distances between two Mo atoms are 3.4 Å and between the Mo and the mono-, bi-, and tridentate O atoms are 1.8, 2.1, and 2.3 Å, respectively. The contour level of the $2F_{obs} - F_{calc}$ and the anomalous $F^+ - F^-$ difference electron density map is 3.5σ and 21.0σ, respectively. (B) Binding site of the Mo_3 cluster represented as polyhedron. The binding site is built up by the loop following strand α3 and helices α3a and α3b of all three α subunits (see Figure S1, Supporting Information).

deviations of the X−Mo−X angle up to ±20° from the ideal value of 90°.

Besides the mentioned two covalent bonds, multiple hydrogen bonds are formed between the Mo_8 cluster and the polypeptide scaffold frequently mediated by solvent molecules (Figure S2B, Supporting Information). For example, Hisα130 points onto two edge-shared O atoms and Hisα114 interacts with the terminal O atom of the displaced octahedron coordinated to Gluα129. Proα153 and Proα154 contribute to

dx.doi.org/10.1021/ja303084n | J. Am. Chem. Soc. 2012, 134, 9768−9774

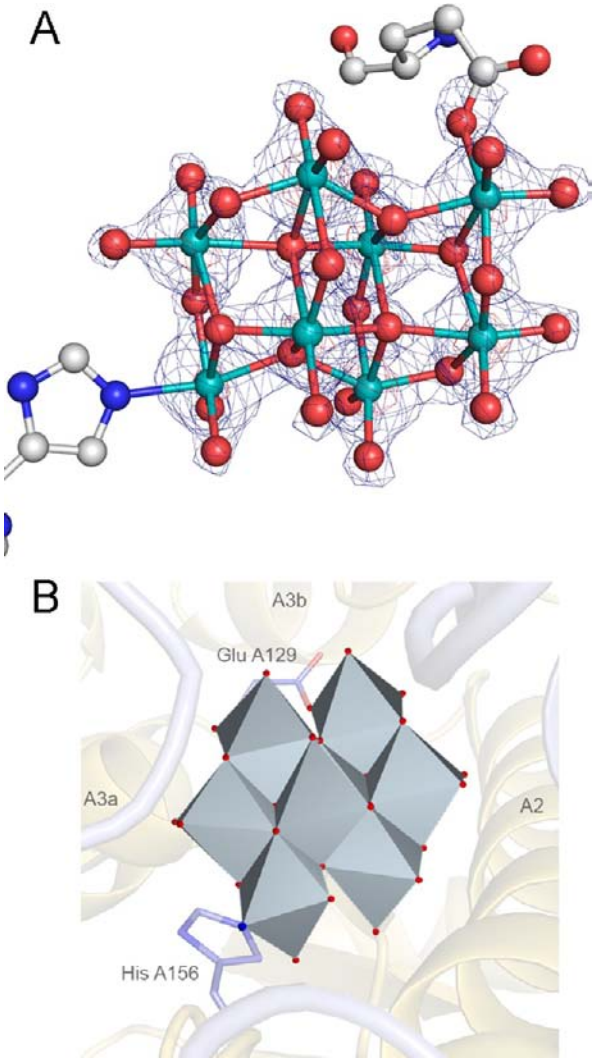

Figure 3. The covalent Mo_8 cluster. (A) Structure with $2F_{obs} - F_{calc}$ and $F^+ - F^-$ electron densities (contour level 3.0σ and 15.0σ, respectively). Two Mo atoms are coordinated to the $O_{\varepsilon 1}$ oxygen atom (red) of Gluα129 and to the $N_{\varepsilon 2}$ nitrogen atom (blue) of Hisα156. The distances between bridged Mo atoms are 3.2−3.4 Å and between Mo and the monodentate, bidentate, tridentate, and tetradentate O atoms are 1.8, 2.0, 2.1, and 2.2 Å, respectively. The Mo−N distance is 2.2 Å. (B) Binding site of the Mo_8 cluster. The binding site is located between helix α2 and strand α3, and between the segments that link helix α3b and strand α4 and helix α3a and strand α3.

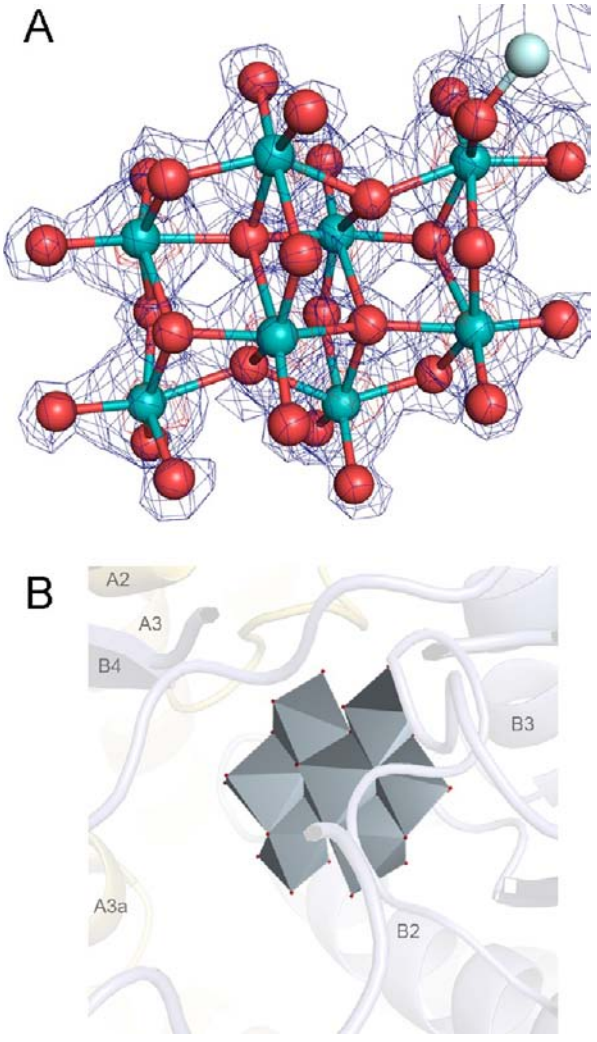

Figure 4. The noncovalent Mo_8 cluster. (A) Structure with $2F_{obs} - F_{calc}$ and $F^+ - F^-$ electron densities (contour level 1.5σ and 7.0σ, respectively). The distances between bridged Mo atoms are 3.2−3.4 Å and between Mo and the monodentate, bidentate, tridentate, and tetradentate O atoms are 1.9, 2.0, 2.2, and 2.0−2.4 Å, respectively. A tentatively fitted Mg^{2+} ion is drawn in light blue. (B) The binding site of the noncovalent Mo_8 cluster is built up by the loops following strands β3 and β4, helix β3, and strand α4.

the unusual loop conformation that significantly determines the shape of the cluster pocket. In the anomalous difference Fourier electron density map (data set MoSto-ano), a peak adjacent to the Mo_8 cluster was, according to its height, tentatively interpreted as phosphorus or sulfur. This atom is ligated in a distorted tetrahedral manner by three O atoms shared with three Mo atoms and one monodentate O atom; the latter interacts with Proα103 and Serα107 (Figure S2B, Supporting Information). Its proximity to Hisα130 and Hisα156 suggests the binding of a phosphate (or sulfate) prior to the synthesis of the covalent Mo_8 cluster.

The Noncovalent Mo_8 Clusters. Three further octamolybdate clusters (Figure 4A), each embedded between subunits α and β (Figure 4B), are termed as noncovalent Mo_8 clusters to distinguish them from the covalent Mo_8 clusters described above. Surprisingly, the noncovalent Mo_8 cluster has virtually the same structure ($[Mo_8O_{28}H_n]^{n-8}$) as the covalent one at the obtained resolution, but might be more protonated due to its noncovalent attachment. It is also fully occupied with the temperature factor of the molybdenums being 9.9 ± 1.7 $Å^2$. The degree of distortion between the MoO_6 octahedra and the distances between Mo and O atoms also correspond to those of the covalent Mo_8 cluster.

The noncovalent cluster is characterized by significantly more interactions to the protein scaffold as its covalent counterpart (Figure S2C, Supporting Information), a few of them being highlighted. Two prolines (Proβ150, Proβ151) and three glycines (Glyβ127, Glyβ128, Glyβ130) largely determine the geometry of the pocket and partly shield the cluster, in particular, one of the displaced MoO_n octahedra, from bulk solvent. Most remarkably, the second MoO_n octahedron with three highly nucleophilic O atoms is not stabilized by interactions with amino acids but is instead weakly coordinated to the Mo_{5-7} cluster (see below). Unexpectedly, an additional metal ion seems to be involved in cluster binding. Because of

dx.doi.org/10.1021/ja303084n | J. Am. Chem. Soc. 2012, 134, 9768−9774

the height of the electron density, the absence of an anomalous signal, its octahedral ligation shell, and the metal−O distance, a Mg^{2+} ion is an attractive candidate (it is present at a concentration of 1 mM in the protein solution). The putative Mg^{2+} ion is chelated to three monodentate O atoms from different MoO_n octahedra, one solvent oxygen atom, and the two main chain carbonyl oxygen atoms of Serβ147 and Metβ149. Another remarkable structural feature involves three consecutive histidines that participate in binding of the noncovalent Mo_8 cluster (Figure S2C, Supporting Information). Hisα156, bonded to the covalent Mo_8 cluster, acts as a linker between the two Mo_8 clusters; Hisα157 stabilizes the O atoms of one of the displaced MoO_n octahedra, and Hisα158 fills a gap between the polypeptide and the cluster. It is obvious that at higher pH values these histidines become deprotonated, and, consequently, their interactions to the negatively charged clusters become weakened. This conclusion is substantiated by "solution studies" with MoSto demonstrating that pH increase causes cluster degradation and molybdate release.[26]

The Mo_{5-7} Clusters. Three Mo_{5-7} clusters (Figure 5A) are located between subunits α and β (one per each dimer) (Figure 5B), however, comparatively distant from the protein surface of the cavity. Their electron densities reveal an inhomogeneous Mo composition interpreted as superposition of several POM clusters whose ratio varies between different crystals. In the applied crystal Mosto-hres, the occupancy of the equatorial Mo in the pentagonal plane is, indicated by values between 0.4 and 0.5, relatively uniform, while occupancy of the axial MoO_n octahedron linked to the noncovalent Mo_8 cluster is ca. 0.3 and that of the exposed axial MoO_n octahedron is ca. 0.2 (Figure 5A). Architecturally, the core of the Mo_{5-7} cluster can be described as distorted $(Mo)Mo_5$ building block as found in larger clusters.[4] Accordingly, the five equatorial MoO_n octahedra are mutually corner-linked and share edges either with the MoO_7 unit directed to the noncovalent Mo_8 cluster or with the exposed MoO_7 unit, thus pretending a Mo_7 cluster. The resulting composition of the $Mo(Mo)_5$ cluster might be $[Mo_6O_{27}H_n]^{n-18}$ (Figure 5A). Alternatively, the electron density can be interpreted as partial Mo_5 cluster generated by degrading the Mo_6 cluster or as partial Mo_7 cluster consisting of the Mo_6 cluster linked with the solvent-exposed axial molybdate.

Contact between the Mo_{5-7} cluster and the polypeptide is solely provided by Proα131 and perhaps by Lysβ153 whose side chain is highly disordered due to the limited occupancy of the cluster (Figure S2D, Supporting Information). In addition, the Mo_{5-7} cluster interacts via several solvent molecules with two covalent Mo_8 clusters. The high solvent accessibility of the Mo_{5-7} cluster is compatible with its low occupancy and inhomogeneity within the crystal.

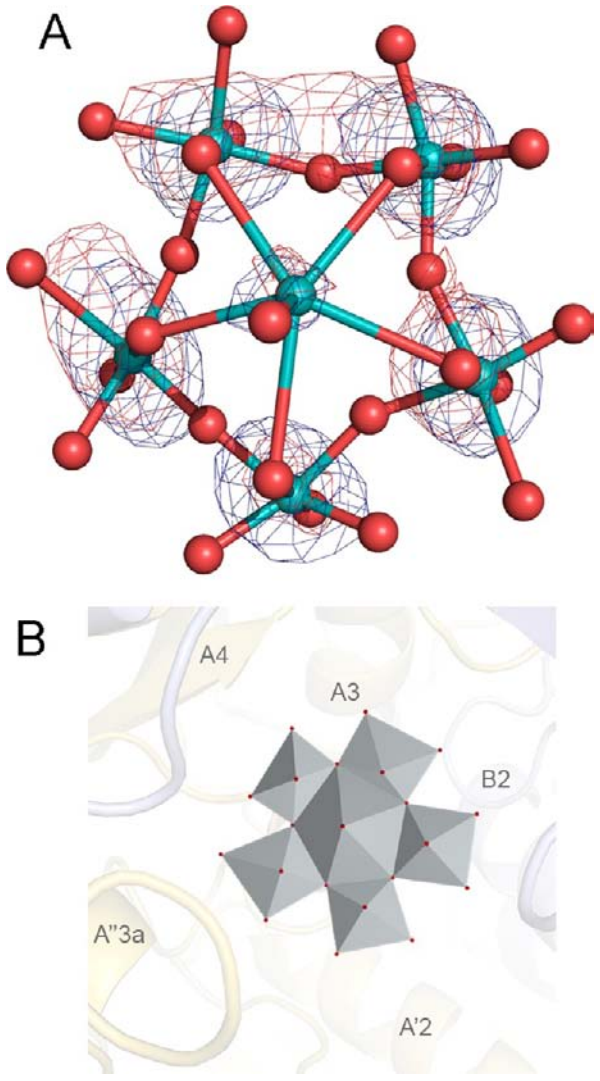

Figure 5. The Mo_{5-7} cluster. (A) Structure of the distorted $Mo(Mo)_5$ cluster with $2F_{obs} - F_{calc}$ and $F^+ - F^-$ electron densities (contour level 1.0σ and 3.0σ, respectively). The weakly occupied axial Mo directed to bulk solvent was omitted. The distances between bridged equatorial Mo atoms are on average 3.4 Å and between equatorial and axial Mo atoms 3.3 Å. Because of the low occupancy of this cluster, the O atoms are not visible in the electron density in contrast to those of the other clusters. (B) The binding site of the Mo_{5-7} cluster is positioned closer to the cavity center. It is weakly attached to helix β2, to the segment following strand β4, to the two linkers connecting helix α3 and strand α4 as well as helix β3 and strand β4, and to other polyoxomolybdate clusters mostly via solvent molecules.

3. DISCUSSION

To correlate individual features of each protein surface contacting a POM cluster with basic template, nucleation/condensation, catalyst, and protection properties, we postulate for MoSto two border scenarios that define a frame of POM cluster formation. On one side, small clusters, which are spontaneously and transiently formed under bulk conditions (representing a virtual library of building blocks), are selectively stabilized by the protein matrix in a subsequent step by binding and protecting them (shielding against hydrolysis). An indirect influence of the protein on the formation of small clusters is possible, if special electrostatic conditions in the solvent-filled cavity promote self-assembly processes. On the other side, the polypeptide directly governs the formation of larger clusters by determining the cluster type (acting as template), by promoting the polymerization reaction (acting as nucleation site or even as catalyst for the condensation process), and also by binding and protecting the formed POM cluster. In the latter case, protein-induced synthesis and stabilization are spatially and temporally not separable. The formation of each cluster type proceeds within these two scenarios such that the protein-induced and self-assembly contributions differ from cluster to cluster.

The Mo_{5-7} cluster is surrounded to a higher extent by bulk solvent than the other POM clusters (Figure 5). We, therefore, assume that its formation is only slightly conducted by protein-induced factors but predominantly by the inherent self-

assembly power of the (Mo)Mo_5 unit found as building block in Mo_{36},[1,6,10] Mo_{57},[1,10,11] and "Keplerate" type clusters.[1,10,30,31]

The cluster types along the 3-fold symmetry axis are essentially specified by the shape/size/symmetry of the protein surface. These geometrical constraints obviously promote cluster formation; however, the unspecificity of van der Waals contacts results in the simultaneous formation of several cluster types superimposed in the electron density and is therefore not clearly definable. For these clusters, the self-assembly proportion is still high, and the protein matrix rather serves as unspecific template and protector by enveloping the clusters. The Mo_3 cluster is an exception as it is, in addition, covalently bound to three optimally spaced histidine side chains. Although unstable in bulk solvent, Mo_3/W_3 clusters can be obviously stabilized if one of the three terminal oxygens are replaced either (a) by conversion into a bidentate oxygen atom as in $[PMo_{12}O_{40}]^{3-}$ (the famous cluster of the Keggin type[7]), (b) by an exchange into a kinetically more stable ligand as isothiocyanate in the $[W_3S_4(SCN)_9]^{5-}$ cluster,[32] or (c) by proteinogenic ligands as in the case of MoSto (Figure 2).

The asymmetric Mo_8 clusters (not present as building blocks in larger aggregates) are embedded into shallow, asymmetric but not largely shielded pockets (Figures 3 and 4) and presumably formed to a higher extent by a protein-induced process. Template transcription is provided by a large number of specifically positioned polar or charged residues of the polypeptide scaffold that mediates complementarity (and also binding) by multiple interactions with the POM cluster (Figure 2, Supporting Information). Particularly striking are three well-distributed histidines around both Mo_8 clusters, each of them endowed with a specific functionality (see above). Surprisingly, covalent fixation does not significantly affect cluster stability, as indicated by the equally high occupancy of covalent and noncovalent Mo_8 clusters. This statement holds true at least for the conditions of preparation and crystallization applied in this work. Previous solution studies on MoSto revealed a differential cluster degradation/Mo release at increasing pH (6.5−8.0) values,[16,26] suggesting a selective deprotonation of the histidines and thus a different stability of the two Mo_8 clusters.

The protein matrix appears to be more involved in the polymerization reaction of the Mo_3 and the Mo_8 clusters than of the Mo_{5-7} cluster and the larger aggregates at the 3-fold axis. A crucial function can again be attributed to the involved histidines. Their electrophilic properties obviously predestine them to attract nucleophilic monomolybdates, to reduce the repulsion of their negative charges, and thus to position them near to each other. In particular, regarding the Mo_8 clusters synthesis, the histidines may even catalyze the condensation reaction by pointing toward bridging molybdate oxygen atoms, by donating protons, and by neutralizing, after reprotonation by the solvent, the negatively charged clusters via strong ionic hydrogen bonds. The positively charged protein pocket thereby increases the electrophility of the adjacent molybdates and induces further growth. A reversed mechanism, when a growing nucleophilic species attracts an electrophilic group, is assumed for the growth of the "giant POM clusters"[30] and may also take place in the case of the Mo_{5-7} cluster provided that the displaced nucleophilic MoO_n octahedron of the noncovalent Mo_8 cluster acts as a nucleation site.

For depositing more than 100 Mo atoms in a compact but easily accessible form inside the cell, nature has developed a protein capable to synthesize/bind/protect POM clusters. This unique quality of MoSto combines macromolecular biochemistry with supramolecular inorganic chemistry both characterized by a tremendous structural diversity. The thereby generated host/guest system[8] might be exploited by using the protein cavity (host) with its tailor-made pockets as a bioreactor for synthesizing novel POM clusters (guest) in a controllable and tunable way. In principle, there are three basic factors to be modified: (i) the conditions of self-assembly, (ii) the amino acids that coat the cluster binding pockets, and (iii) the type of the metal ion. More specifically, (i) the inherent self-assembly capability of molybdates is reflected in the correspondence between the found protein-bound polyoxomolybdate (or fragments thereof) and building blocks or precursors of larger "bulk" type species arguing for a preferential formation of these species in (protein-free) solution. POM cluster formation in solution can be induced and directed by modifying the pH value, the redox state, and by additional compounds used for nucleation and linkage. (ii) POM cluster formation is further directed by the complex surface functionalities of the protein including global features as size/shape, symmetry, and electrostatics as well as specific local factors like the accurate positions and orientation of amino acid side chains described above. The properties of each cavity pocket can be specifically modified and tailored by site-directed exchanges of the amino acid residues involved. In addition, inorganic compounds like phosphate and Mg^{2+} can bind into the polypeptide pocket, as found in this work, which further enlarges their versatility. (iii) Formation of new POM clusters may also be caused by applying different metal ions or more than one type of metal ion. Comparison between the polyoxomolybdate and polyoxotungstate clusters present in MoSto and in WSto[21] reveals that subtle differences between the metal ions appear to influence the structure of POM clusters in a given binding pocket. While the binding sites and structures of the Mo_3 and W_3 clusters are identical, the W_6 cluster in WSto is positioned in the binding site of the noncovalent Mo_8 cluster in MoSto. Likewise, the binding site of the W_7 cluster (in WSto) is occupied by the covalent Mo_8 cluster (in MoSto). (It has to be considered that in WSto the pockets are only partly occupied with polyoxotungstate.) This metal-dependent template property of the protein confirms the working hypothesis that the polypeptide-assisted and self-assembly processes cooperate synergistically in POM cluster formation, hence making a rational design of novel clusters inside the MoSto bioreactor to a challenge.

4. MATERIALS AND METHODS

Bacterial Strain and Growth Conditions. The bacterial strain used in this study was *A. vinelandii* wild type strain OP (DSM 366; ATCC 13705). Bacteria were grown as described elsewhere.[16] The standard medium contained 10 μM Na_2MoO_4.

Cell Extract Preparation and Protein Purification. The basic conditions applied for the procedures of extract preparation (French press treatment, ultracentrifugation) and MoSto purification including DEAE-Sephacel chromatography, ammonium sulfate fractionation, and Superdex-200 gel filtration were the same as described.[16] However, to improve the protein stability and to avoid unnecessary loss of Mo during preparation, 1 mM ATP, 1 mM $MgCl_2$, and 2 mM Na_2MoO_4 were added to the standard buffer (50 mM MOPS−NaOH, pH 6.5) throughout the isolation and purification procedure. The degree of protein purity was hardly affected by the modified elution conditions. The protein content was determined with the Coomassie Blue reagent according to Bradford.[33]

Structure Analysis of MoSto. Most suitable crystals were obtained using the hanging-drop method at 4 and 10 °C with a drop volume of 1 μL of protein solution containing 5−20 mg mL^{-1}

dx.doi.org/10.1021/ja303084n | J. Am. Chem. Soc. 2012, 134, 9768−9774

MoSto, 50 mM MOPS−NaOH, pH 6.5, 50 mM NaCl, 1 mM ATP, 1 mM $MgCl_2$, 2 mM Na_2MoO_4, and 1 μL of reservoir solution (1 M $(NH_4)_2HPO_4$ and 0.1 M sodium citrate, pH 5.6). Native and anomalous data were collected under cryogenic conditions (ca. 100 K) at the Swiss Light Source (SLS), beamline PXII, Villigen, Switzerland and at the European Synchrotron Radiation Facility (ESRF), beamline ID29, Grenoble, France, respectively. Data processing was performed with the HKL[34] and XDS[35] program suites. Phases were derived from the WSto structure.[21] The MoSto structure was refined with REFMAC5.[36] The polypeptide was manually inspected, and the models for the polyoxomolybdate clusters were built with COOT[37] and O.[38] Anomalous difference Fourier ($F^+ - F^-$) maps were calculated with programs of the CCP4 suite.[39] Figures 1, 2A, 3A, 4A, and 5A were prepared with PyMol (Schrodinger, LLC), and Figures 2B, 3B, 4B, and 5B were prepared with Diamond (Crystal Impact).

PDB Codes. The atomic coordinates and the structure factors for MoSto-hres are deposited in the Protein Data Bank under the accession code 4F6T.

Mo Determination. The content of molybdenum in the purified MoSto protein was routinely determined after buffer change to molybdenum-free 50 mM MOPS (pH 6.5) according to the chemical-catalytic method of Pantaler,[40] modified and adapted for proteins by Fenske et al.[16] The type of metal ion present in MoSto crystals was analyzed by an X-ray fluorescence scan in the wavelength range 0.6−2.1 Å and by a single anomalous dispersion experiment at a wavelength of 1.71 Å both performed at beamline ID29, ESRF.

■ ASSOCIATED CONTENT

Ⓢ Supporting Information

Table S1 includes data collection and refinement statistics. Topology diagrams of subunits α and β of MoSto (Figure S1) and interactions between the polypeptide and the Mo_3, Mo_{5-7}, covalent Mo_8, and noncovalent Mo_8 clusters (Figure S2A−D) presented in a schematic manner. The material is available free of charge via the Internet at http://pubs.acs.org.

■ AUTHOR INFORMATION

Corresponding Author

ulrich.ermler@biophys.mpg.de; klaus.schneider1@uni-bielefeld.de

Author Contributions

[§]These authors contributed equally.

Notes

The authors declare no competing financial interests.

■ ACKNOWLEDGMENTS

We thank Hartmut Michel for financial support and the scientists of the PXII beamline at the Swiss-Light-Source, Villigen, and of the ID29 beamline (Christoph Müller-Dieckmann) in Grenoble for assistance during data collection and X-ray fluorescence experiments.

■ REFERENCES

(1) *Oxomolybdates: From Structures to Functions in a New Era of Nanochemistry*; Müller, A., Roy, S., Eds.; Wiley-VCH: Weinheim, 2004.
(2) Long, D. L.; Tsunashima, R.; Cronin, L. *Angew. Chem., Int. Ed.* **2010**, *49*, 1736.
(3) Hall, N. *Chem. Commun.* **2003**, 803.
(4) Gouzerh, P.; Che, M. *Actual. Chim.* **2006**, *298*, 9.
(5) Müller, A.; Beckmann, E.; Bögge, H.; Schmidtmann, M.; Dress, A. *Angew. Chem., Int. Ed.* **2002**, *41*, 6.
(6) Müller, A.; Botar, B.; Das, S. K.; Bögge, H.; Schmidtmann, A.; Merca, A. *Polyhedron* **2004**, *23*, 2381.
(7) Pope, M. T.; Müller, A. *Angew. Chem., Int. Ed. Engl.* **1991**, *30*, 15.
(8) Müller, A.; Reuter, H.; Dillinger, S. *Angew. Chem., Int. Ed. Engl.* **1995**, *34*, 34.
(9) Fielden, J.; Cronin, L. In *Encyclopaedia of Supramolecular Chemistry*; Atwood, J. L., Steed, J. W., Eds.; Taylor & Francis Group: Columbia, 2005.
(10) Müller, A.; Körgerler, P.; Kuhlmann, C. *Chem. Commun.* **1999**, 1347.
(11) Müller, A.; Meyer, J.; Krickemeyer, E.; Beugholt, C.; Bögge, H.; Peters, F.; Schmidtmann, M.; Kögerler, P.; Koop, M. J. *Chem.-Eur. J.* **1998**, *4*, 1000.
(12) Pope, M. T. *Prog. Inorg. Chem.* **1991**, *30*, 181.
(13) Gourley, D. G.; Schuttelkopf, A. W.; Anderson, L. A.; Price, N. C.; Boxer, D. H.; Hunter, W. N. *J. Biol. Chem.* **2001**, *276*, 20641.
(14) Delarbre, L.; Stevenson, C. E.; White, D. J.; Mitchenall, L. A.; Pau, R. N.; Lawson, D. M. *J. Mol. Biol.* **2001**, *308*, 1063.
(15) Hille, R. *Trends Biochem. Sci.* **2002**, *27*, 360.
(16) Fenske, D.; Gnida, M.; Schneider, K.; Meyer-Klaucke, W.; Schemberg, J.; Henschel, V.; Meyer, A. K.; Knochel, A.; Müller, A. *ChemBioChem* **2005**, *6*, 405.
(17) Hernandez, J. A.; George, S. J.; Rubio, L. M. *Biochemistry* **2009**, *48*, 9711.
(18) Schwarz, G.; Mendel, R. R.; Ribbe, M. W. *Nature* **2009**, *460*, 839.
(19) Pienkos, P. T.; Brill, W. J. *J. Bacteriol.* **1981**, *145*, 743.
(20) Schneider, K.; Müller, A.; Johannes, K. U.; Diemann, E.; Kottmann, J. *Anal. Biochem.* **1991**, *193*, 292.
(21) Schemberg, J.; Schneider, K.; Demmer, U.; Warkentin, E.; Müller, A.; Ermler, U. *Angew. Chem., Int. Ed.* **2007**, *46*, 2408.
(22) Rees, D. C.; Akif Tezcan, F.; Haynes, C. A.; Walton, M. Y.; Andrade, S.; Einsle, O.; Howard, J. B. *Philos. Trans. R. Soc., A* **2005**, *363*, 971.
(23) Bursakov, S. A.; Gavel, O. Y.; Di Rocco, G.; Lampreia, J.; Calvete, J.; Pereira, A. S.; Moura, J. J.; Moura, I. *J. Inorg. Biochem.* **2004**, *98*, 833.
(24) Briozzo, P.; Evrin, C.; Meyer, P.; Assairi, L.; Joly, N.; Barzu, O.; Gilles, A. M. *J. Biol. Chem.* **2005**, *280*, 25533.
(25) Meyer, P.; Evrin, C.; Briozzo, P.; Joly, N.; Barzu, O.; Gilles, A. M. *J. Biol. Chem.* **2008**, *283*, 36011.
(26) Schemberg, J.; Schneider, K.; Fenske, D.; Müller, A. *ChemBioChem* **2008**, *9*, 595.
(27) Yamashita, I.; Iwahori, K.; Kumagai, S. *Biochim. Biophys. Acta* **2010**, *1800*, 846.
(28) Lewin, A.; Moore, G. R.; Le Brun, N. E. *Dalton Trans.* **2005**, 3597.
(29) Lipscomb, W. N. *Inorg. Chem.* **1965**, *4*, 132.
(30) Müller, A.; Krickemeyer, E.; Bögge, H.; Schmidtmann, M.; Peters, F. *Angew. Chem., Int. Ed.* **1998**, *37*, 3360.
(31) Long, D. L.; Cronin, L. *Chemistry* **2006**, *12*, 3698.
(32) Müller, A.; Fedin, V. P.; Diemann, E.; Bögge, H.; Krickemeyer, E.; Sölter, D.; Giuliani, A. M.; Barbieri, R.; Adler, P. *Inorg. Chem.* **1994**, *33*, 2243.
(33) Bradford, M. M. *Anal. Biochem.* **1976**, *72*, 248.
(34) Kabsch, W. *J. Appl. Crystallogr.* **1993**, *26*, 795.
(35) Otwinowski, Z.; Minor, W. *Methods Enzymol.* **1997**, *276*, 307.
(36) Murshudov, G. N.; Vagin, A. A.; Dodson, E. J. *Acta Crystallogr., Sect. D: Biol. Crystallogr.* **1997**, *53*, 240.
(37) Emsley, P.; Cowtan, K. *Acta Crystallogr., Sect. D: Biol. Crystallogr.* **2004**, *60*, 2126.
(38) Jones, T. A.; Zou, J. Y.; Cowan, S. W.; Kjeldgaard, M. *Acta Crystallogr., Sect. A* **1991**, *47*, 110.
(39) Potterton, E.; McNicholas, S.; Krissinel, E.; Cowtan, K.; Noble, M. *Acta Crystallogr., Sect. D: Biol. Crystallogr.* **2002**, *58*, 1955.
(40) Pantaler, R. P. *J. Anal. Chem. USSR* **1963**, *18*, 519.